Available online at www.sciencedirect.com
ScienceDirect
Journal of Molecular Catalysis A: Chemical 270 (2007) 56–60
JOURNAL OF MOLECULAR CATALYSIS A: CHEMICAL
www.elsevier.com/locate/molcata

Photoinduced decomposition of $BaFeO_3$ during photodegradation of methyl orange

Yang Yang, Yinshan Jiang *, Yingwei Wang, Yanbin Sun

Key Laboratory of Automobile Materials, Ministry of Education, Department of Materials Science and Engineering, Jilin University, Changchun 130026, PR China

Received 24 February 2006; received in revised form 12 January 2007; accepted 14 January 2007
Available online 24 January 2007

Abstract

Photodegradation of methyl orange under UV light irradiation has been studied over a photocatalyst $BaFeO_3$ prepared by the citrate–nitrate combustion method. Both X-ray diffraction (XRD) and Fourier transform infrared (FTIR) spectroscopy have revealed the decomposition of the structure of $BaFeO_3$ after the photocatalytic experiment. The photoinduced decomposition of $BaFeO_3$ is due to the existence of unstable iron ions in $BaFeO_3$. X-ray photoelectron spectroscopy (XPS) indicates that the valence state of iron ions in $BaFeO_3$ changes after the photocatalytic experiment. SEM observation shows that the morphology of $BaFeO_3$ does not change under UV light irradiation. It is indispensable to select a suitable element for the B-site in order to synthesize photostable perovskite photocatalysts.

Keywords: Perovskite; Photocatalysis; Photostability

1. Introduction

Perovskite oxides with the general formula of ABO_3 are frequently encountered in inorganic chemistry. An ideal perovskite has an ABO_3 stoichiometry and a cubic crystal structure which is composed of a three-dimensional framework of corner-sharing BO_6 octahedra. BO_6 octahedron is often considered as the basic unit of perovskite structure [1]. Furthermore most of the properties of perovskite oxides are related to the network of BO_6 octahedra [2] and the state of B-site cations [3,4].

Perovskite compounds with the general formula of ABO_3 exhibit a wide range of ferro-, piezo-, and pyro-electrical properties as well as electro-optical effects which make them suitable as electronic, structural, magnetic, and refractory materials [5]. Moreover, perovskites have been used as catalysts for controlled partial hydrocarbon oxidation [6], gaseous pollutant removal [7,8], oxidative dehydrogenation of alkanes [9] and photocatalysis [10]. Especially, the use of perovskites as photocatalysts is particularly attractive because of their narrower band gap [11] (often less than 3.0 eV) which can be easily excited under visible light or UV light irradiation. As a promising photocatalyst perovskite has been studied extensively in the field of decomposition of water under UV and visible light irradiation ($BaZn_{1/3}Nb_{2/3}O_3$ and $BaCo_{1/3}Nb_{2/3}O_3$, etc. [12–16]) and photoinduced degradation of organic pollutants (ordinary perovskite $SrTiO_3$ [17] and layered perovskite $La_2Ti_2O_7$ [18]).

Mills and Hunte argue that it is more meaningful to investigate the intrinsic mechanism of photocatalysis and related photochemical reaction than to find new photocatalysts [19]. However, researchers still focus their attention on designing novel photocatalysts [20,21], because the progress in designing new photocatalysts can help us understand the nature of photocatalysis and photoinduced chemical reaction thoroughly and vice versa. In this paper we design a novel perovskite photocatalyst ($BaFeO_3$) and discuss the photocatalytic property and the photostability of oxides of this kind. It is believed that better understanding of the photoinduced decomposition of $BaFeO_3$ can help us in designing photostable photocatalyst in the future.

* Corresponding author at: College of Material Science and Engineering, Jilin University, 6, West-Minzhu Avenue, Changchun 130026, PR China. Tel.: +86 431 8502234; fax: +86 431 8502234.
E-mail addresses: jiangyinshan@163.com, jiangyinshan@126.com (Y. Jiang).

1381-1169/$ – see front matter © 2007 Elsevier B.V. All rights reserved.
doi:10.1016/j.molcata.2007.01.033

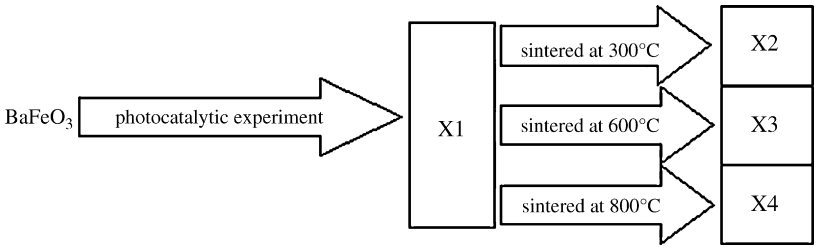

Fig. 1. The illustration of experimental procedure.

2. Experimental

2.1. Materials

For the preparation of $BaFeO_3$, ferric nitrate (A.R.98.5%), barium nitrate (A.R.99.5%), citric acid (A.R.99.8%), ammonia solution (A.R.25.0–28.0%), methyl orange (A.R.) and deionized water were used.

2.2. Sample preparation

$BaFeO_3$ was synthesized by the citrate–nitrate combustion method. In the process of synthesizing precursor gel, 0.1 mol L^{-1} well-mixed metal nitrates solution in the stoichiometric ratio was prepared and after blending completely 0.5 mol L^{-1} citric acid (the molar ratio of citric acid/metal ions ≈ 1) were dropped into the mixed solution. In order to combine citric acid with metal ions adequately, pH of the mixed solution was kept at 9 (with the help of aqueous ammonia) and the temperature was maintained at 70 °C. Furthermore the mixture was constantly stirred during the whole process. The mixed solution was then polymerized under infrared irradiation for more than 10 h till gel-like precursor was formed. The gel-like precursor was calcined at 450 °C for 2 h to burn off the organic ingredient and then at 800 °C for 4 h to form the perovskite structure.

2.3. Photocatalytic properties experiment

Photocatalytic degradation of methyl orange was carried out in a homemade reactor equipped with a 250 W high-pressure mercury lamp. Before photocatalytic experiments, 20 mL of methyl orange solution (20 mg L^{-1}) containing 0.01 g photocatalyst was well mixed and the absorbency of original methyl orange solution (namely A_0) was determined on a UV-754 UV–vis spectrophotometer at 464 nm. During the photocatalytic process, the absorbencies of methyl orange solution (namely A_i) were measured every 10 min. The photocatalytic decolorization rates of methyl orange were computed via the formula: $d = (A_0 - A_i)/A_0$.

After the photocatalytic experiment, the photocatalysts were filtrated and calcined at different temperatures (300, 600 and 800 °C) for 4 h. A schematic diagram of the experimental process is given in Fig. 1. X1 represents the intermediate phase substance filtrated after the photocatalytic experiment. X2–X4 respectively represent the product obtained by calcination of X1 at 300, 600 and 800 °C for 4 h.

2.4. Characterization methods

X-ray diffractograms were collected on a Rigaku D/MAX 2500PC diffractometer (Cu/50 kV/250 mA, 2θ from 20° to 60°) and FTIR spectra were obtained with a Nexus-670 FTIR spectrometer. SEM micrographs were recorded with a JEM-2000FX (JEOL Ltd.) scanning electron microscope (operated at 20 keV). XPS spectra were recorded with a Perkin-Elmer PHI-5300 ESCA (Al mono, 22.2 W, 18.0 μ, 45.0°).

3. Results and discussion

3.1. Structure characterization

Black powder of $BaFeO_3$ has been synthesized by the citrate–nitrate combustion method. Fig. 2 shows the XRD pattern of the $BaFeO_3$ powder. The sample is well crystallized and most of the diffraction peaks can be indexed as perovskite $BaFeO_3$ except a few peaks of $BaCO_3$ impurity which is regarded as inevitable in the process of synthesizing perovskites [22,23].

Photoinduced decomposition of $BaFeO_3$ after the photocatalytic experiment is shown in Fig. 3 (the XRD pattern of X1). It can be seen from Fig. 3 that the crystallized structure is only $BaCO_3$ without any other diffraction peaks and it is indicated that $BaFeO_3$ decomposes accompanying the photoinduced degradation of methyl orange. It is obvious that there is no

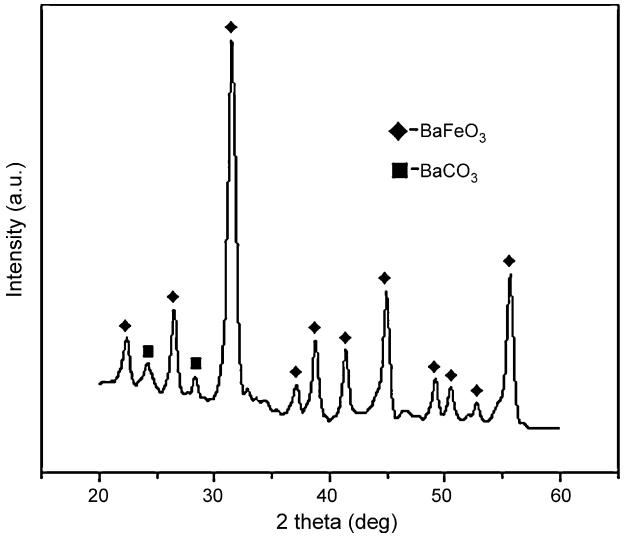

Fig. 2. The XRD pattern of $BaFeO_3$: (♦) $BaFeO_3$; (■) $BaCO_3$.

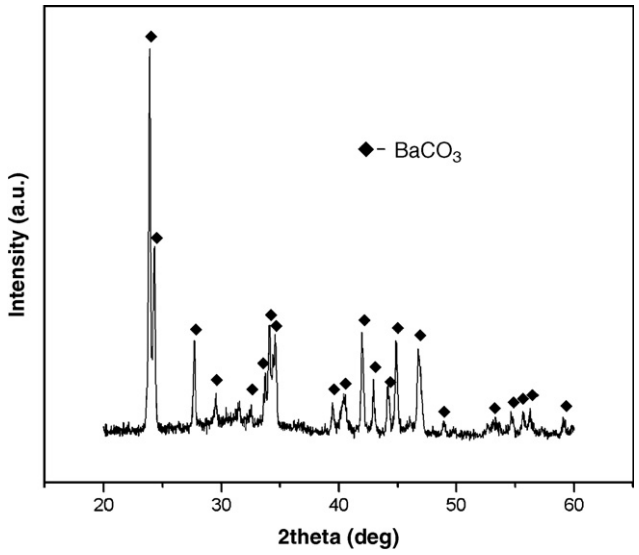

Fig. 3. The XRD pattern of X1: (♦) $BaCO_3$.

evident existence of crystallized Fe-containing substances in Fig. 3. So it is supposed that during the process of photocatalytic degradation of methyl orange a photochemical reaction between $BaFeO_3$ and CO_2 (released from the photodegradation of methyl orange) is induced under UV light irradiation. Being excited by UV light irradiation, $BaFeO_3$ reacts with CO_2 and decomposes to an intermediate phase (namely X1) which is composed of $BaCO_3$ and an Fe-containing amorphous substance. With regard to the unsteadiness of a certain kind of perovskite structure, Salje claims that the most outstanding feature of the perovskite structure is thermodynamically extremely stable from the view of topology whereas its actual crystal structure appears to be very unstable [24]. Our findings fall in with his viewpoint.

Fig. 4(a)–(c) represents the XRD pattern of X2, X3 and X4, respectively. (a) shows that X2 is composed of $BaCO_3$ with a trace of poorly crystallized $BaFe_2O_4$. (b) shows that X3 is a

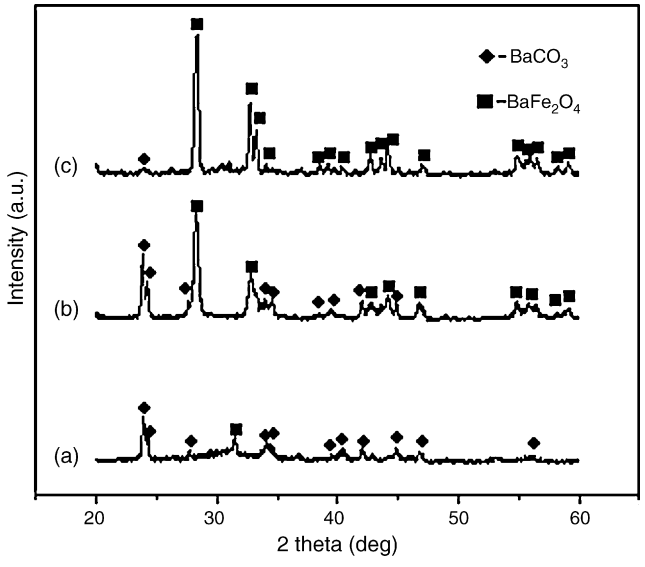

Fig. 4. The XRD patterns of X2–X4: (a) X2; (b) X3; (c) X4; (♦) $BaCO_3$; (■) $BaFe_2O_4$.

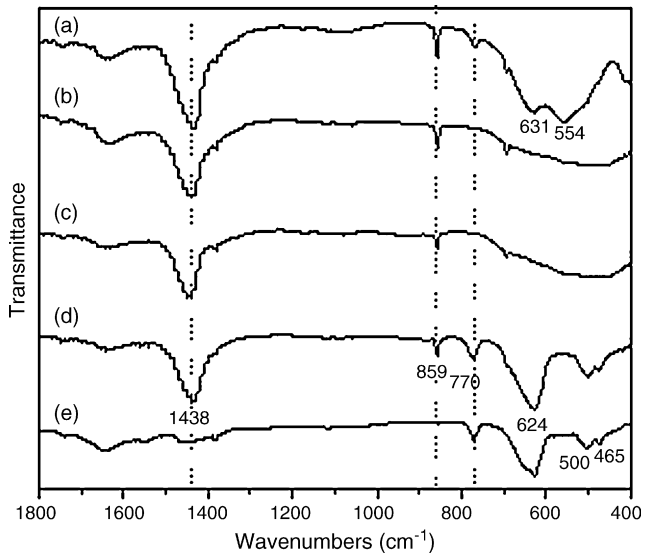

Fig. 5. The FTIR spectra of the samples: (a) $BaFeO_3$; (b) X1; (c) X2; (d) X3; (e) X4.

mixture of $BaCO_3$ and $BaFe_2O_4$. After calcining X1 at 800 °C, its composition is completely transformed to $BaFe_2O_4$ as shown in (c). Through comparing (a), (b) and (c) it can be confirmed that the composition of the intermediate phase (namely X1) is $BaCO_3$ and Fe-containing amorphous substance which are gradually transformed to $BaFe_2O_4$ by calcination up to 800 °C.

Theoretically, we should obtain $BaFeO_3$ instead of $BaFe_2O_4$ after calcining X1 at 800 °C, which indicates that some of Ba^{2+} ions are lost during the calcination.

Fig. 5(a)–(e) represents the FTIR spectra of $BaFeO_3$, X1–X4, respectively. Through comparing FTIR spectra and XRD patterns it can be found that the main IR bands of $BaFeO_3$ at 631 and 554 cm^{-1} [25] tremendously decrease, which indicates the photoinduced decomposition of $BaFeO_3$ during the photocatalytic experiment. It is also obvious that the main IR bands of $BaCO_3$ at 1438 and 859 cm^{-1} decrease accompanying the increase in the intensity of IR bands of $BaFe_2O_4$ at 770, 624, 500 and 465 cm^{-1}. It indicates the intermediate phase is gradually transformed to $BaFe_2O_4$ by calcination up to 800 °C. XRD and FTIR results are in accord with each other and show a structural transformation of $BaFeO_3$ during the photocatalytic experiment.

3.2. Photocatalytic property

Photocatalytic decolorization curve of methyl orange is given in Fig. 6 and the slope of this curve reflects the rate of photocatalytic reaction. The decolorization rate curve can be divided into two parts: the steep slope of the curve between 0 and 10 min reflects a high rate of the photocatalytic reaction, and the slope of the curve between 10 and 120 min is much less steep than the former. The photocatalytic decolorization of methyl orange is a cumulative process with the decolorization curve growing continuously. The break of the curve at 10 min reflects the photoinduced decomposition of photocatalyst $BaFeO_3$ and with decreasing amount of $BaFeO_3$ the photocatalytic reaction rate decreases as reflected in a mild slope of the curve between 10

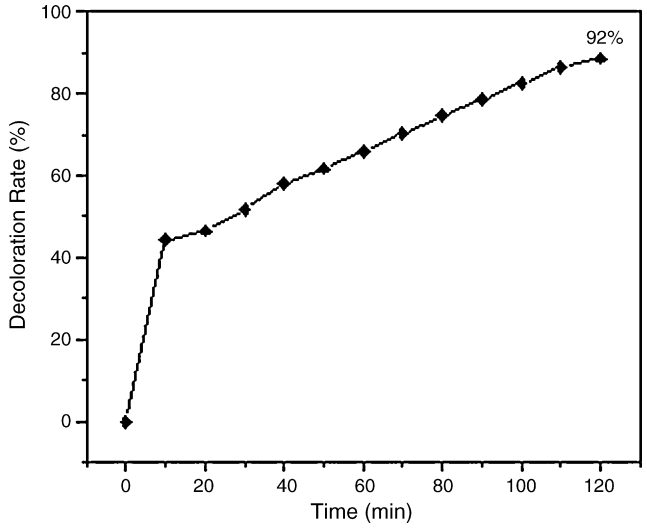

Fig. 6. The time course of photocatalytic decolorization of methyl orange using $BaFeO_3$ as a photocatalyst.

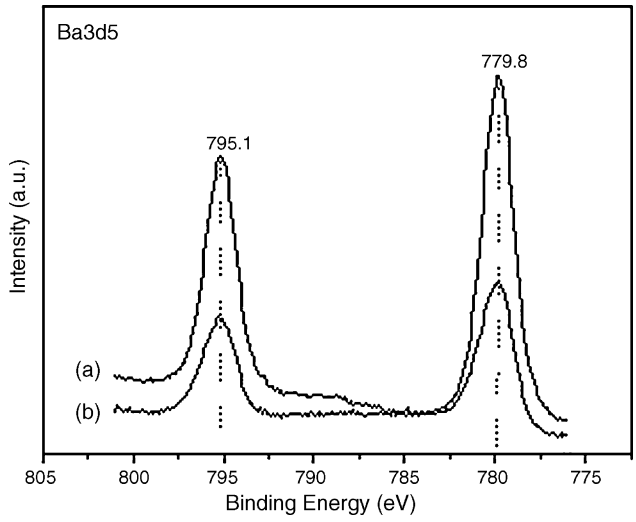

Fig. 7. The XPS spectra of Ba $3d_5$ in $BaFeO_3$ and X1: (a) $BaFeO_3$; (b) X1. The binding energy of 779.8 eV corresponds to Ba^{2+}.

and 120 min in Fig. 6. After UV light irradiation for 120 min the photocatalytic decolorization of methyl orange reaches 92%. The high photocatalytic degradation rate indicates that $BaFeO_3$ has excellent photocatalytic activity which stems from the special crystal structure of perovskite $BaFeO_3$ with FeO_6 octahedra. We have discussed the cause of high photocatalytic activity of $BaFeO_3$ in another paper [26]. The whole process of the photocatalytic degradation of methyl orange over perovskite $BaFeO_3$ can be summarized as follows:

$$\text{photocatalyst}\,BaFeO_3 + h\nu \rightarrow e^- + h^+ \quad (1)$$

$$e^- + h^+ + H_2O + \text{methyl orange} \rightarrow \text{micromolecular organic} + CO_2 \quad (2)$$

$$\text{photocatalyst}\,BaFeO_3 + CO_2 \rightarrow BaCO_3 + \text{Fe-containing amorphous substance} \quad (3)$$

In reaction (1) $BaFeO_3$ absorbs photons and produces electron–hole pairs under the UV light irradiation. Then reaction (2) represents the photoinduced reaction between methyl orange and electron–hole pairs. According to the conventional photocatalytic mechanism [27] the decolorization of methyl orange is due to the oxidizing reaction between h^+ (and other oxiding base groups) and the chromatic group in methyl orange. The poor photostability of $BaFeO_3$ as a photocatalyst is reflected in reaction (3).

3.3. XPS analysis

Fig. 7(a) shows the XPS spectrum of Ba $3d_5$ in $BaFeO_3$ and (b) that of Ba $3d_5$ in X1. It can be seen that the binding energy of Ba $3d_5$ shows no difference between Fig. 7(a) and (b), indicating that the valence state of barium do not change during the photocatalytic experiment. The binding energy of 779.8 eV corresponds to Ba^{2+}.

Fig. 8(a) shows the XPS spectrum of Fe 2p in $BaFeO_3$ and (b) that of Fe 2p in X1. The binding energy of 724.7 and 711.1 eV in (a) shift respectively to 724.0 and 710.9 eV in (b). The binding energy of 710.9 eV in (b) corresponds to Fe^{3+} and 711.1 eV in (a) may correspond to Fe^{4+}.

According to XPS spectral analysis it can be deduced that the photoinduced structural transformation and poor photostability of photocatalyst $BaFeO_3$ are due to the valence state change of iron ions in $BaFeO_3$ which is induced by UV light irradiation during the photocatalytic reaction.

3.4. SEM observation

Fig. 9(a) and (b) shows the morphology of $BaFeO_3$ and X1 respectively and it can be seen that the two samples have similar conglomerate states. Thus it is indicated that the photocatalytic

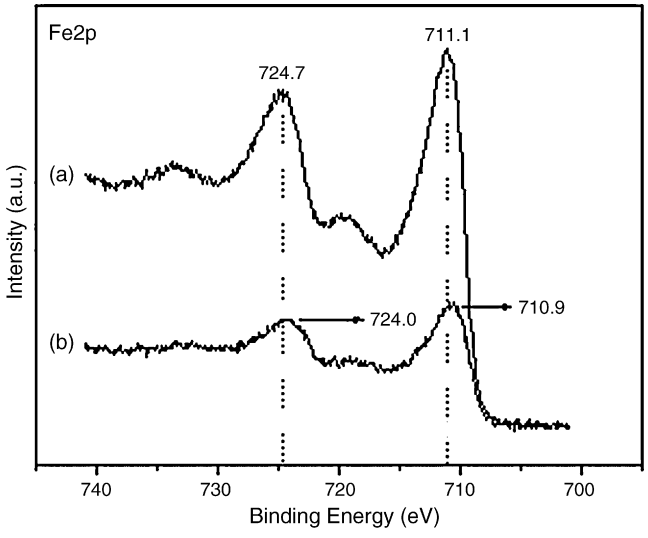

Fig. 8. The XPS spectra of Fe 2p in $BaFeO_3$ and X1: (a) $BaFeO_3$; (b) X1. The binding energy of 710.9 eV in (b) corresponds to Fe^{3+}. The binding energy of 711.1 eV in (a) corresponds to Fe^{4+}.

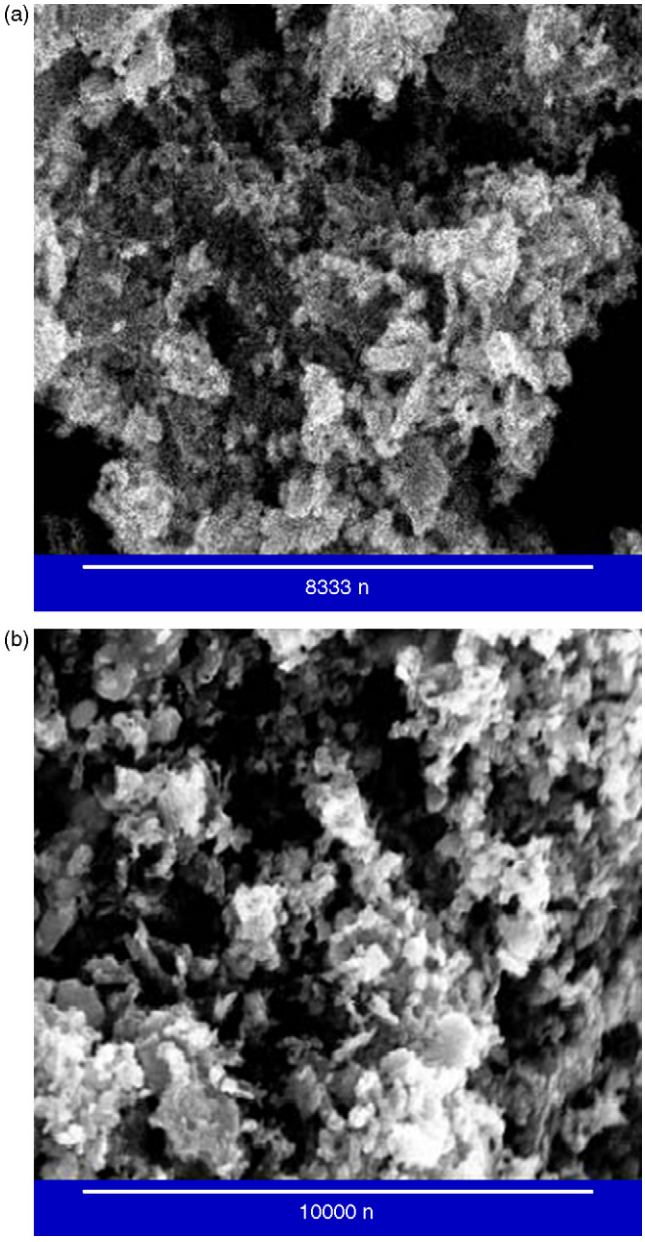

Fig. 9. (a) The SEM micrograph of $BaFeO_3$; (b) the SEM micrograph of X1.

reaction and UV light irradiation have no obvious influence on the morphology of the sample.

4. Conclusions

Photocatalytic experiments show that $BaFeO_3$ is a novel photocatalyst with excellent photocatalytic property which is due to the redox ability of electron–hole pairs produced by FeO_6 octahedra in the perovskite structure. Both XRD and FTIR analyses prove that perovskite $BaFeO_3$ has poor photostability, which is due to the changeable valence state of iron ions in the structure. XPS spectra confirms the transition of the valence state of iron ions in $BaFeO_3$. UV light irradiation has no obvious influence on the morphology of the sample. It is indispensable to select a suitable stable element in the B-site in order to synthesize stable perovskite photocatalysts.

Acknowledgements

This work is supported by Project 985-Automotive Engineering of Jilin University and the National Nature Science Foundation of China (grant no. 50574043).

References

[1] L. Tan, L. Yang, X. Gu, W. Jin, L. Zhang, N. Xu, J. Membr. Sci. 230 (2004) 21.
[2] K. Kuzushita, S. Morimoto, S. Nasu, Physica B 329–333 (2003) 736.
[3] M. Misono, Catal. Today 100 (2005) 95.
[4] F.M.M. Snijkers, A. Buekenhoudt, J. Cooymans, J.J. Luyten, Scripta Mater. 50 (2004) 655.
[5] H. Tanaka, M. Misono, Curr. Opin. Solid State Mater. Sci. 5 (2001) 381.
[6] W.F. Libby, Science 171 (1971) 499.
[7] L.A. Pedersen, W.F. Libby, Science 176 (1972) 1355.
[8] N. Guihaume, S.D. Peter, M. Primet, Appl. Catal. B 10 (1996) 325.
[9] Z.M. Fang, Q. Hong, Z.H. Zhou, S.J. Dai, W.Z. Weng, H.L. Wau, Catal. Lett. 61 (1999) 39.
[10] F.T. Wagner, G.A. Somorjai, Nature 285 (1980) 599.
[11] J. Yin, Z. Zou, J. Ye, J. Phys. Chem. B 107 (2003) 61.
[12] C. He, O. Yang, Ind. Eng. Chem. Res. 42 (2003) 419.
[13] A. Kudo, H. Kato, S. Nakagawa, J. Phys. Chem. B 104 (2000) 571.
[14] J. Yin, Z. Zou, J. Phys. Chem. B 107 (2003) 61.
[15] K. Domen, J.N. Kondo, M. Hara, T. Tanaka, Bull. Chem. Soc. Jpn. 73 (2000) 1307.
[16] H. Kato, A. Kudo, J. Phys. Chem. B 105 (2001) 4285.
[17] S. Ahuja, T.R.N. Kutty, J. Photochem. Photobiol. A: Chem. 97 (1996) 99.
[18] D.W. Hwang, K.Y. Cha, J. Kim, H.G. Kim, S.W. Bae, J.S. Lee, Ind. Eng. Chem. Res. 42 (2003) 1184.
[19] A. Mills, S.L. Hunte, J. Photochem. Photobiol. A: Chem. 108 (1997) 1.
[20] S. Tokunaga, H. Kato, A. Kudo, Chem. Mater. 13 (2001) 4624.
[21] D. Dvoranova, V. Brezova, M. Mazur, M.A. Malati, Appl. Catal. B 37 (2002) 91.
[22] O.A. Harizanov, Mater. Lett. 34 (1998) 232.
[23] I. Maclaren, C.B. Ponton, J. Eur. Ceram. Soc. 20 (2000) 1267.
[24] B. Salje, Phil. Trans. R. Soc. Lond. A 328 (1989) 409.
[25] C.O. Augustin, L. John Berchmans, R. Kalai Selvan, Mater. Lett. 58 (2004) 1260.
[26] Y. Yang, Y. Sun, Y. Jiang, Mater. Chem. Phys. 96 (2006) 234.
[27] A. Fujishima, K. Honda, Nature 238 (1972) 37.